AGU PUBLICATIONS

JGR

Journal of Geophysical Research: Oceans

RESEARCH ARTICLE
10.1002/2015JC011251

Special Section:
Forum for Arctic Modeling and Observational Synthesis (FAMOS): Results and Synthesis of Coordinated Experiments

Vertical scales and dynamics of eddies in the Arctic Ocean's Canada Basin

Mengnan Zhao[1] and Mary-Louise Timmermans[1]

[1]Department of Geology and Geophysics, Yale University, New Haven, Connecticut, USA

Key Points:
- Mooring measurements in the Arctic's Canada Basin reveal a range of mesoscale eddy types
- Eddies at intermediate depths have two cores with each core showing anomalous water properties
- Double-core eddies have origins at a water mass front separating Arctic Eurasian and Canadian Water

Correspondence to: M. Zhao,
mengnan.zhao@yale.edu

Citation:
Zhao, M., and M.-L. Timmermans (2015), Vertical scales and dynamics of eddies in the Arctic Ocean's Canada Basin, J. Geophys. Res. Oceans, 120, 8195–8209, doi:10.1002/2015JC011251.

Received 18 AUG 2015
Accepted 18 NOV 2015
Accepted article online 23 NOV 2015
Published online 19 DEC 2015

Abstract A decade of moored measurements from the Arctic Ocean's northwestern Beaufort Gyre (collected as a component of the Beaufort Gyre Exploration Project) are analyzed to examine the range of mesoscale eddies over the water column and the dynamical processes that set eddy vertical scales. A total of 58 eddies were identified in the moored record, all anticyclones with azimuthal velocities ranging from 10 to 43 cm/s. These are divided into three classes based on core depths. Shallow eddies (core depths around 120 m) are shown to be vertically confined by the strong stratification of the halocline; typical thicknesses are around 100 m. Deep eddies (core depths around 1200 m) are much taller (thicknesses around 1300 m) owing to the weaker stratification at depth, consistent with a previous study. Eddies centered around mid-depths all have two cores (vertically aligned and separated in depth) characterized by velocity maxima and anomalous temperature and salinity properties. One core is located at the base of the halocline (around 200 m depth) and the other at the depth of the Atlantic Water layer (around 400 m depth). These double-core eddies have vertical scales between those of the shallow and deep eddies. The strongly decreasing stratification in their depth range motivates a derivation for the quasi-geostrophic adjustment of a nonuniformly stratified water column to a potential vorticity anomaly. The result aids in interpreting the dynamics and origins of the double-core eddies, providing insight into transport across a major water mass front separating Canadian and Eurasian Water.

1. Introduction

Eddies are ubiquitous in the ocean, and contribute to ocean stirring and mixing, transporting heat, nutrients, and other water properties [e.g., Flor, 2010; Mathis et al., 2007; Nishino et al., 2011; Watanabe et al., 2014]. Eddies provide an important link between ocean basin boundaries and the interior, and the study of their properties and origins can shed light on the variability of their originating boundary currents and fronts. This has been shown in the Arctic Ocean where mesoscale eddies at all depths in the water column have been observed and studied, with the most prevalent eddy types being eddies in the Canada Basin halocline, mostly centered between around 30 and 300 m depth [e.g., Hunkins, 1974; Newton et al., 1974; Manley and Hunkins, 1985; D'Asaro, 1988; Padman et al., 1990; Muench et al., 2000; Pickart et al., 2005; Spall et al., 2008; Pickart and Stossmeister, 2008; Timmermans et al., 2008; Zhao et al., 2014; Watanabe et al., 2014]. Study of these eddies has provided insight into boundary current instabilities and halocline ventilation processes [e.g., Pickart et al., 2005; Pickart and Stossmeister, 2008; Spall et al., 2008], baroclinic instability of surface fronts [e.g., Timmermans et al., 2008], and transport of biological species [e.g., Watanabe et al., 2014].

In a recent study, Zhao et al. [2014] analyzed Ice-Tethered Profiler (ITP, www.whoi.edu/itp) [Krishfield et al., 2008] data to obtain a synthesis of the Arctic-wide halocline eddy field sampled over a decade from 2004. Eddies were found to be dominated by cold-core anticyclones with horizontal scales comparable to the first baroclinic deformation radius (~8 to 14 km from the Eurasian Basin to the Canadian Basin) [Zhao et al., 2014]. Halocline eddy azimuthal velocities ranged between 10 cm/s and more than 30 cm/s, and lifetimes were estimated to be from months to years. The distribution of eddies (127 in total) satisfied a robust relationship between the eddy thickness-to-radius ratio (H/R) and the ambient water column stratification N (where $N^2 = -\frac{g}{\rho_0}\frac{\partial \rho}{\partial z}$ is the buoyancy frequency, and ρ_0 is a reference density) around the depth level of the eddy cores, with $H = R/f \cdot N$, where f is the Coriolis parameter [Zhao et al., 2014]. This is consistent with the dynamical adjustment of the water column to a potential vorticity anomaly [e.g., Carpenter and Timmermans, 2012]. Mean eddy thicknesses in the Canada Basin halocline were found to be around 95 m

[Zhao et al., 2014]. In the Canada Basin, the shallowest eddies were consistent with origins related to instability of a surface front in the northern sector of the basin, while deeper halocline eddies (most prevalent in the southwestern basin) were likely generated by instability of boundary currents associated with Pacific Water inflows.

Much deeper anticyclones in the Canada Basin, centered ~1200 m depth, have been measured by a mooring in a region just northeast of the Chukchi Borderlands [Carpenter and Timmermans, 2012]. Carpenter and Timmermans [2012] put forward a formation mechanism for these eddies by dense outflows from the Chukchi Borderland region into the more strongly stratified Canada Basin interior. They showed that dynamical adjustment of the weak ambient water stratification at depth in the basin results in tall eddies with thicknesses ~1300 m. Shallower than this, warm-core anticyclones have been sampled at ~400 m depth in the Atlantic Water layer (e.g., Y. Bebieva and M.-L. Timmermans, An examination of double-diffusive processes in a mesoscale eddy in the Arctic Ocean, submitted to Journal of Geophysical Research, 2015), although they are less prevalent than the other eddy types.

While a variety of eddy types have been examined in the Canada Basin, this analysis is motivated by our observation of a new type of eddy that has not one azimuthal velocity maximum in the vertical (as do the halocline and deep eddies described above) but two maxima separated by a depth range of weaker azimuthal velocity. They are also characterized by anomalous core temperature and salinity properties at the depths of each of the azimuthal velocity maxima. We explain the origins and dynamics of these eddies (which we refer to as double-core eddies), and set them in context with the properties of other eddies. We show how double-core eddies have influence throughout multiple water mass layers.

The range of eddy types (at all depths) is investigated here through an analysis of moored measurements in the northwest Canada Basin. We analyze temperature, salinity, pressure, and velocity data from a mooring deployed as part of the Beaufort Gyre Exploration Project (BGEP, http://www.whoi.edu/beaufortgyre) [Proshutinsky et al., 2009]. Mooring measurements as well as hydrographic data used to supplement the moored measurements are described in section 2, where we also describe the regional water masses relevant to the variety of eddies studied here. In section 3, we summarize the range of eddy types sampled by the mooring, focusing our attention on the group of distinct double-core eddies. The vertical structure of eddy azimuthal velocity is analyzed in context with the ambient water stratification in section 4; this requires an extension of the formalism of Carpenter and Timmermans [2012] to account for nonuniform ambient water stratification. A possible formation mechanism for the double-core eddies is then put forward. Our results are summarized and discussed in section 5.

2. Measurements and Water-Column Structure

2.1. Moored Measurements

We analyze data from 2003 to 2012 from one of 4 BGEP moorings (Mooring B) deployed in the Canada Basin (at 78°N, 150°W, to the northeast of the Northwind Ridge, Figure 1a). In addition to other instrumentation, the mooring includes a McLane Moored Profiler (MMP) profiling between ~50 m (to avoid deeper ice keels closer to the surface) and ~2050 m with water-column profiles of the two components of horizontal velocity, temperature, salinity, and pressure at profiling intervals of 6 and then 48 h [Proshutinsky et al., 2009]. Data have a vertical resolution of 2 dbar.

Mooring B sampled more mesoscale eddies (at all depths) than any of the other three BGEP moorings [Carpenter and Timmermans, 2012], likely because it is situated in the vicinity of complex topography and near the confluence of boundary currents of Pacific and Atlantic origin. Further, the region will be shown to be of particular relevance to the double-core eddies. The extensive depth range of the MMP profiles allows for a comprehensive analysis of different classes of eddies over (effectively) the full water column, and the velocity measurements provide essential information on eddy dynamics. Although the sample location is restricted, the 9 year duration of the mooring record to some extent guarantees that the majority of eddy types in the Beaufort Gyre region are sampled.

2.2. Hydrographic Measurements

To supplement the mooring measurements and aid in interpretation of eddy origins, CTD data from the World Ocean Database (WOD) and the Chukchi Borderland Expedition in 2002 (CBL2002) are analyzed;

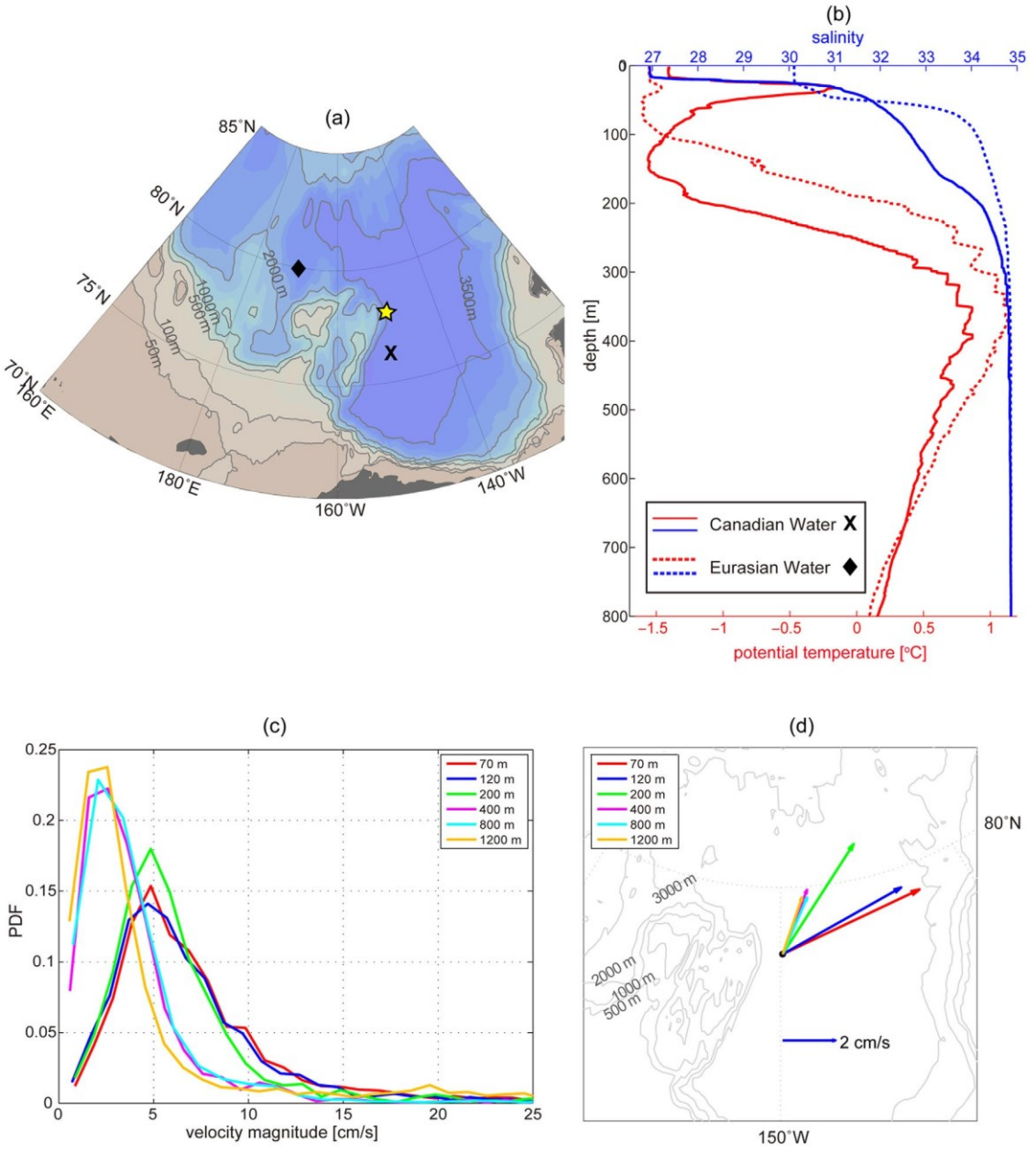

Figure 1. (a) Map of the Canada Basin showing the bathymetry in the vicinity of Mooring B (marked by the yellow star). (b) Typical Canadian Water profile (solid lines) on 27 August 2002 at the location marked by the black cross in Figure 1a, and typical Eurasian Water profile (dashed lines) on 31 August 2002 at the location marked by the black diamond in Figure 1a. Potential temperature (ϑC) profiles are red and salinity profiles are blue. (c) Probability density function (PDF) of velocity magnitude (cm/s) for the entire Mooring B record at the depths shown (bin size 1 cm/s); (d) time-averaged velocity over August 2003 to August 2012 at the depths shown for the Mooring B record excluding eddies.

these cover the western Canada Basin and Chukchi Borderland/Mendeleev Ridge complex region. WOD CTD profiles include data from buoys, ships, and other instruments (including Ice-Tethered Profilers) and are available from the National Oceanic Data Center: https://www.nodc.noaa.gov/OC5/WOD13. Given spatial and temporal limitations of the hydrographic data in the region, we consider WOD CTD profiles from 1993 to 2012 to obtain a sufficiently comprehensive picture of water mass distributions. CBL2002 data were downloaded from ftp://pscftp.apl.washington.edu/CBL2002Archive/CBLCTDandBottledataasjoa.

2.3. Regional Water Masses

The basic temperature-salinity (T-S) structure in the Canada Basin in the vicinity of Mooring B (Figure 1b, solid lines) is as follows. Below the surface mixed layer are water masses of Pacific Ocean origin that

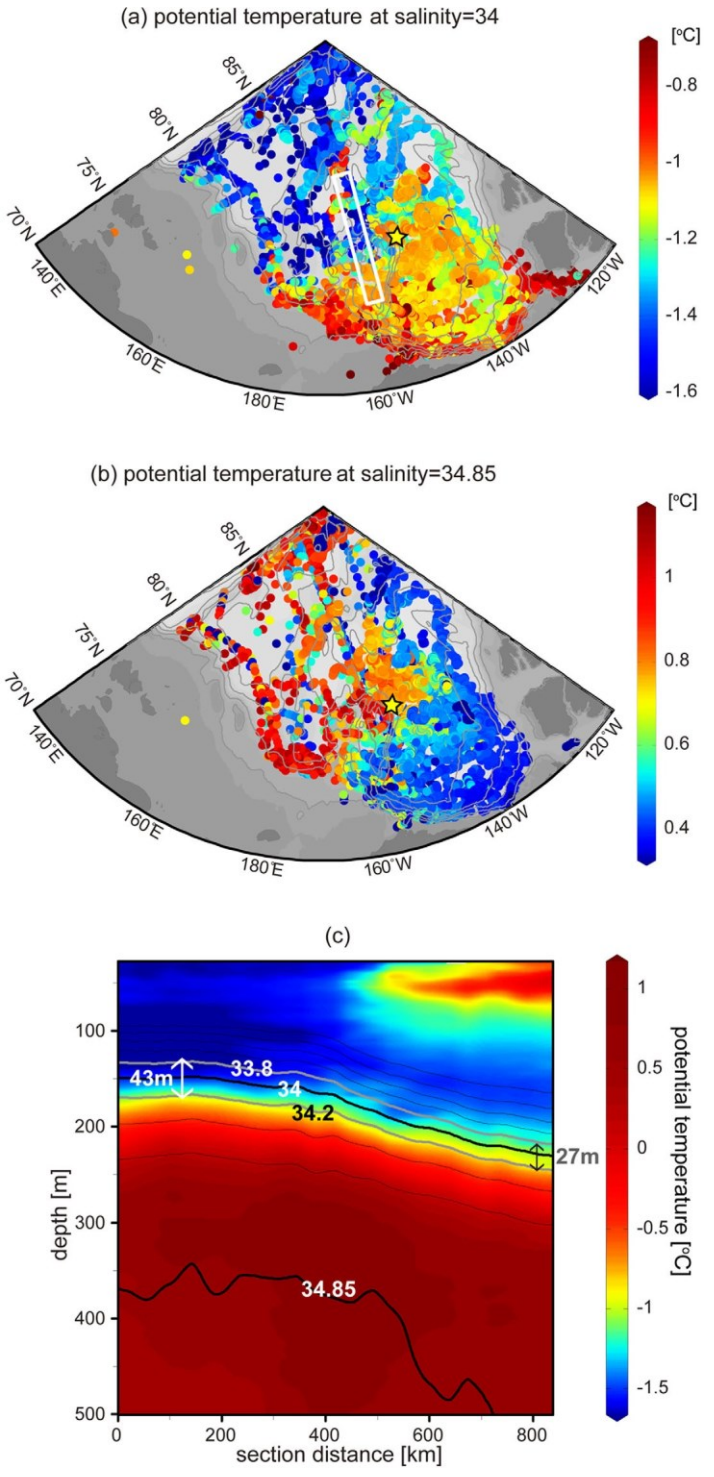

Figure 2. Potential temperature (°C) at (a) S = 34 and (b) S = 34.85 from WOD data between 1993 and 2012 and CBL2002 CTD measurements. The yellow star indicates the location of Mooring B. (c) Potential temperature (°C) section across the Eurasian/Canadian Water front (at ~400 km), with Eurasian Water on the left (the section is from CTD measurements in 2000 and is from north (left) to south, shown by the white frame in Figure 2a). Isohalines are also shown at intervals of 0.2, with grey lines marking S = 33.8 and S = 34.2 encompassing the shallow core water of the mid-depth eddies; temperature has little effect on density at these low temperatures, and isohalines follow the same structure as isopycnals.

comprise the halocline. The shallowest Pacific Summer Water has two branches: Alaskan Coastal Water (S ≈ 31–32) around 50 m and Bering Strait Water (typically with S ≈ 32–33) at ~100 m depth, although the strengths and depths of these branches differ in time and region and sometimes only one branch exists; recent years have seen some changes in these water masses [e.g., Timmermans et al., 2014]. The deeper Pacific Winter Water, modified over the Chukchi Sea in winter, centers around 150 m, with T ≈ −1.5°C and S ≈ 33 [e.g., Coachman et al., 1975]. The basic velocity structure (to be discussed in the next section) shows a clear separation between these upper water layers and deeper water (Figure 1c). Atlantic Water lies below the Pacific Water layers, with a core at ~400 m depth (with T ≈ 0.8°C and S ≈ 34.85). This structure represents the typical Canadian Water column, distinct from the Eurasian Water column with its cold halocline (Figure 1b, dashed lines). The Eurasian Water sees little influence from warm Pacific inflows and is colder (with temperatures around −1.5°C) in the lower halocline (S ≈ 34) compared to the Canadian Water [e.g., Aagaard et al., 1981].

The distribution of water masses shows the Canadian Water (i.e., Pacific Water influence) to the west of Mooring B in the southern part of the Chukchi Borderland/Mendeleev Ridge region (Figure 2a). The higher temperature at S ≈ 34 in this region (of relevance to the double-core eddies, as will be shown later) has been attributed to mixing between the cool Pacific Winter Water and warmer upwelled Atlantic Water over the Chukchi Shelf [see

Woodgate et al., 2005]. The Eurasian Water characterized by the cold halocline is observed to the north of this region.

There is a general cooling pattern of the Atlantic Water temperature maximum (on S 5 34.85) from west to east (Figure 2b), implying the path of the Atlantic Water (and its intrusions) from the boundary regions to the east. Woodgate et al. [2007] examined the Atlantic Water temperature in the region from 1993 to 2002 (see their Figure 2), and concluded a general warming trend over this time, but that the Atlantic Water in the northern Chukchi Borderland/Mendeleev Ridge region shows large variations in temperature possibly owing to the complex topography (and therefore circuitous topographically steered Atlantic Water boundary current) in the region.

The distinguishing properties between Canadian and Eurasian Waters naturally constitute a front along their boundary (Figure 2c). On the Eurasian side of the front, the halocline is cooler compared to the Canadian Water side, while the core of the Atlantic Water layer is warmer and shallower. Eddies can be generated by baroclinic instability of the front, which we will show in section 4.2.1 is particularly relevant to the formation and dynamics of the double-core eddies.

3. Eddy Classification and Properties

Eddies are detected by the presence of large horizontal speeds accompanied by isopycnal displacements and T-S anomalies. Based on past findings, we set this speed criterion to be 10 cm/s [e.g., Hunkins, 1974; Padman et al., 1990; Zhao et al., 2014]. This critical speed is significantly faster than the typical background flow speeds at the mooring site (i.e., geostrophic, tidal, and wind-driven flows). Velocity magnitudes for the entire 9 year mooring record show median values rv5 cm/s at shallow depths (<200 m) and rv2 cm/s at depths >200 m (Figure 1c). Median values are less than 0.7 cm/s slower when profiles with speeds >10 cm/s are removed from the record before the calculation. In most instances of speeds above the threshold of 10 cm/s, anomalous eddy core T-S properties and isopycnal displacements are prominent (Figures 3a and 3b; these features were employed for the detection of eddies by Zhao et al. [2014] in the absence of velocity information). The temperature and salinity of an eddy core are taken to be where the isopycnal field shows the most pronounced displacement and largest potential temperature anomaly from the ambient water. The measured eastward and northward velocities as well as isopycnal displacements (with a convex-lens shape for anticyclones) clearly show the rotational directions of eddies sampled. When speeds faster than 10 cm/s are not accompanied by obvious isopycnal displacements or anomalous temperature, it is possible that an eddy edge skirted the mooring and its core was not sampled. Tidal currents may be another source of large velocities. Although the semidiurnal tidal flows are not well resolved by the Mooring B MMP profiling pattern, previous studies suggest tidal flows are smaller than 10 cm/s in the vicinity of Mooring B, with semidiurnal tidal currents in the region typically around 2 cm/s [Kowalik and Proshutinsky, 1994; Pluedde-mann et al., 1998]. Eddies appear to contribute to most of the kinetic energy of the water column (Figure 3).

Eddies can be categorized into three classes based on their depth ranges (Figure 4): shallow eddies at depths above 200 m, mid-depth eddies between about 200 and 1000 m, and deep eddies with core depths below 1000 m. A total of 31 shallow eddies (e.g., Figures 4a and 4d), 6 mid-depth eddies (e.g., Figures 4b and 4e) and 21 deep eddies (e.g., Figures 4c and 4f) were sampled by Mooring B between August 2003 and August 2012. All eddies are anticyclones, consistent with the predominance of anticyclones documented in past studies. The reason for the much larger proportion of anticyclones compared to cyclones in the Canada Basin remains unclear; elsewhere in the world ocean, Chelton et al. [2011] show that anticyclones dominate the field of long-lived eddies (i.e., in general, anticyclones decay more slowly than cyclones).

Eddy core T-S (Figure 5) indicate different source waters and likely also formation mechanisms for the three classes of eddies. Most shallow eddies have anomalously cold cores (Figure 5, blue triangles), with their core T-S indicating origins of instability of Pacific Winter Water boundary currents (eddies with core salinities around 33), and instability of a northern Canada Basin surface front with fresher core salinity and near-freezing temperature, as found in multiple previous studies [e.g., Pickart et al., 2005; Pickart and Stossmeister, 2008; Timmermans et al., 2008; Zhao et al., 2014]. Three shallow eddies have warm cores (Figure 5, blue triangles warmer than 20.5°C), possibly sourced from Pacific Summer Water boundary currents [Pickart and Stossmeister, 2008; Zhao et al., 2014]. Deep eddies in the record were those analyzed by Carpenter and

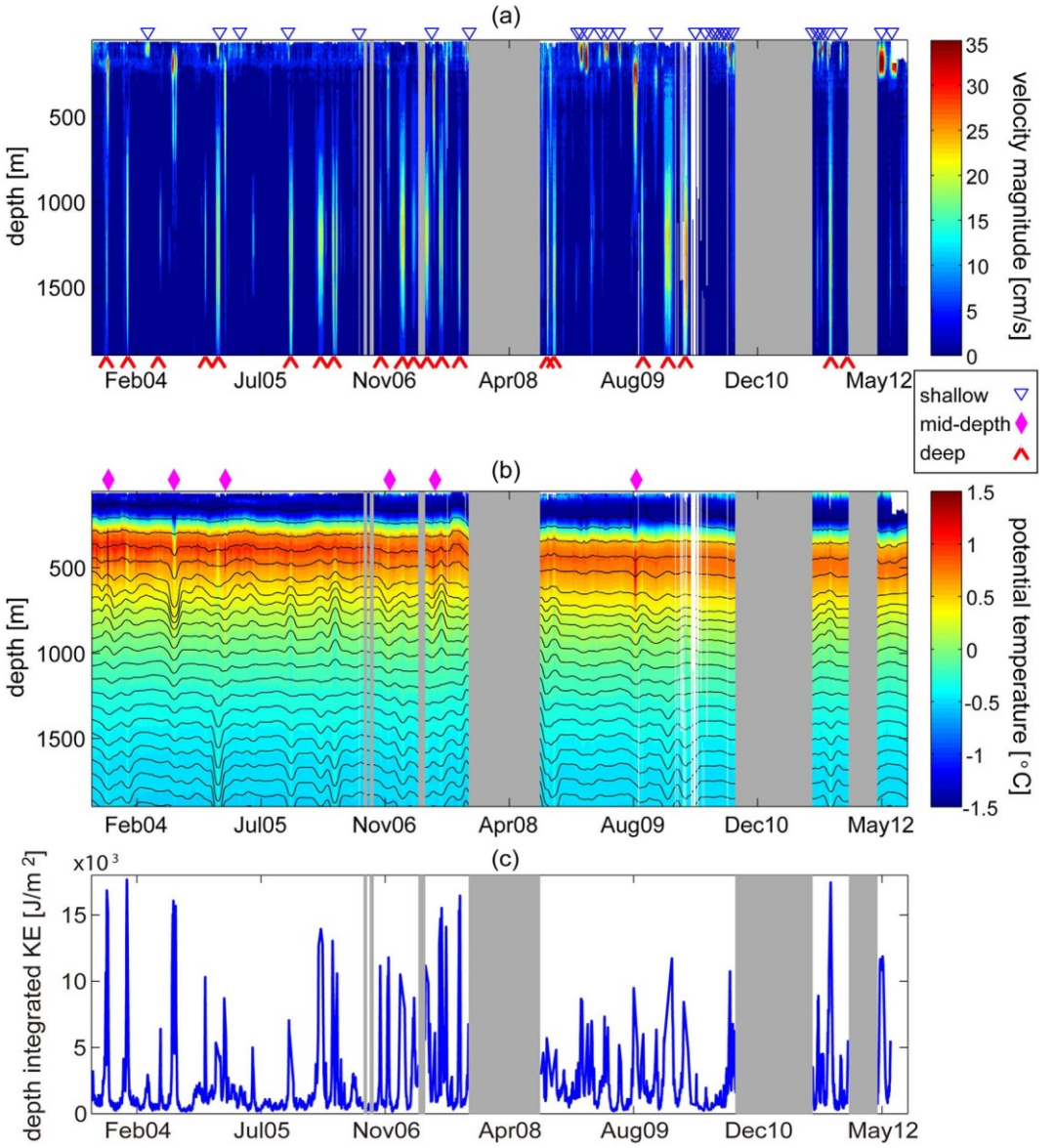

Figure 3. (a) Horizontal velocity magnitude (cm/s) and (b) potential temperature (δC) from Mooring B sampled from August 2003 to August 2012. Isopycnals are shown in Figure 3b chosen to have equal intervals of 80 m at the first profile. The grey areas indicate time ranges without measurements. The high-velocity regions, anomalous temperature, and convex-shaped isopycnal displacements indicate the presence of an eddy; blue triangles mark shallow eddies, magenta diamonds mark mid-depth eddies, and red ticks mark deep eddies. (c) Depth integrated kinetic energy $\int_{\delta} \frac{1}{2}\rho(u^2 + v^2)dz$ (J/m^2) from 64 to 1967 m.

Timmermans [2012], hypothesized to form by dense outflows from the Chukchi Borderland region, as described earlier.

Mid-depth eddies sampled at Mooring B extend from the bottom of the Pacific Winter Water layer to the bottom of the Atlantic Water layer. All have unusual structures compared to the majority of anticyclones sampled; in contrast to the shallow and deep eddies, they all have two (horizontal) velocity maxima in depth, one at the base of the halocline (rv200 m) and the other in the Atlantic Water layer (Figure 6). We refer to the entire (anticyclonic) structure as a single double-core eddy. To our knowledge, these eddies have not been studied before in the Canada Basin, although it is likely that similar features would have been sampled in previous studies if measurements extended deeper [see e.g., Hunkins, 1974]. In the Eurasian Basin, however, an eddy with two distinct cores (vertically aligned and centered at rv300 and rv500 m depth) containing core water from each of two branches of Atlantic Water was identified by Dmitrenko et al.

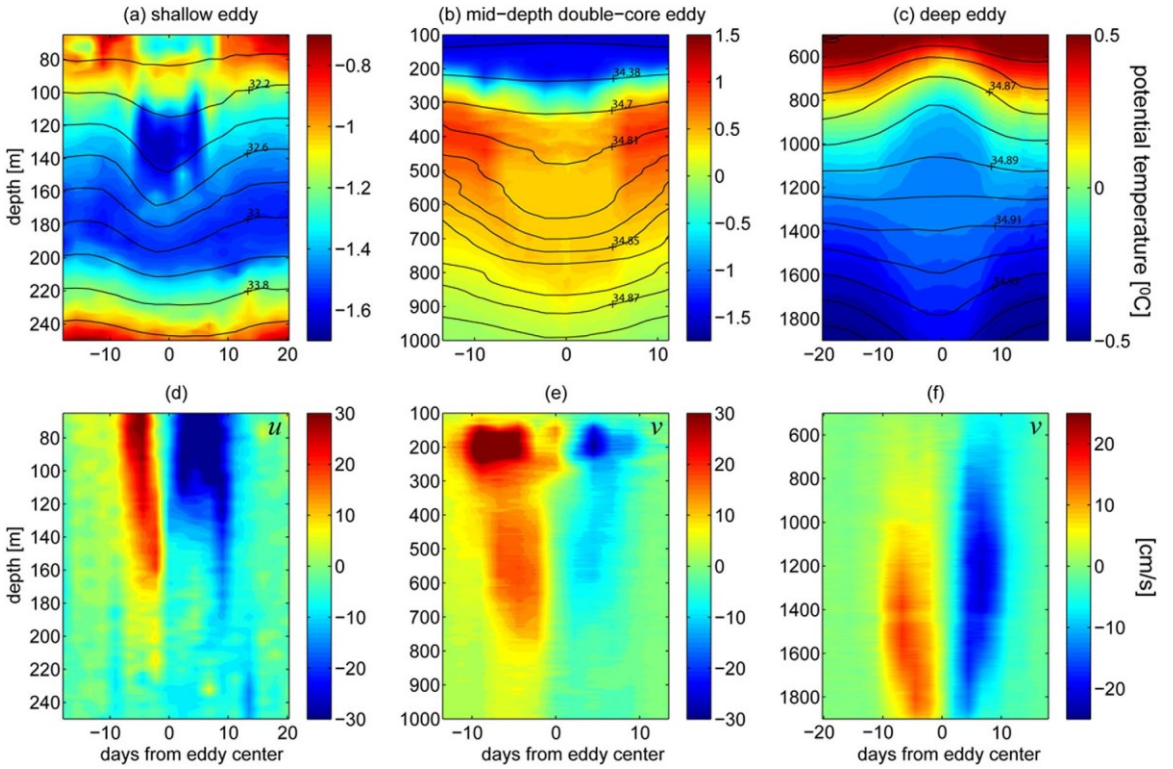

Figure 4. (top row) Potential temperature (ßC) with isohalines overlain for an example (a) shallow eddy (sampled around 25 April 2009), (b) mid-depth eddy (sampled around 23 July 2004), and (c) deep eddy (sampled around 30 April 2006). (bottom row) Horizontal velocity (eastward u or northward v components (cm/s)) for the eddies shown in the top row ((d) shallow, (e) mid-depth, and (f) deep).

[2008], and believed to be generated by instabilities of a Kara Sea front separating the two Atlantic Water masses. A few midlatitude studies document eddies with two distinct cores stacked vertically. For example, Prater and Sanford [1994] show measurements of a Mediterranean eddy, while Lilly and Rhines [2002] show anticyclones in the Labrador Sea, all with two distinct lenses of anomalous temperature and salinity, vertically aligned; formation mechanisms are not elaborated upon in these studies.

The shallow cores of the double-core eddies (Figure 5, green diamonds) are anomalously cold with core temperatures rv21.4ßC and salinities rv34, consistent with Eurasian Water properties at the base of the halocline (Figure 5, dashed line). Deep cores (Figure 5, green squares) have either anomalously cold or anomalously warm waters, centering around the Atlantic Water layer with deep core salinity rv34.85. The T-S properties of the shallow cores suggest origins in the Eurasian Water in the northern region of the Mendeleev Ridge/Chukchi Borderland complex (Figure 2), near the Eurasian/Canadian Water boundary. The heterogeneous Atlantic Water temperature in the region (see section 2.3) is consistent with both the anomalously cool and warm deeper core water, and possible formation mechanisms are discussed in the next section.

4. Vertical Adjustment

Each class of eddy has a different vertical scale with eddies centered on weak stratification being taller than eddies confined in the vertical by strong stratification (Figure 3). In this section, we explore the dynamical adjustment of the water column to eddies, which first requires an assessment of eddy radii.

4.1. Eddy Horizontal Scales

To estimate eddy radii, the moored measurements spaced in time at a single location must be translated to space, which requires knowledge of how fast an eddy translates past the mooring. It is generally understood that a single eddy self-propagates due to the variation in the Coriolis parameter with latitude (i.e., beta-drift) and/or is advected by the background flow (for a comprehensive review see Flor [2010]); dipole

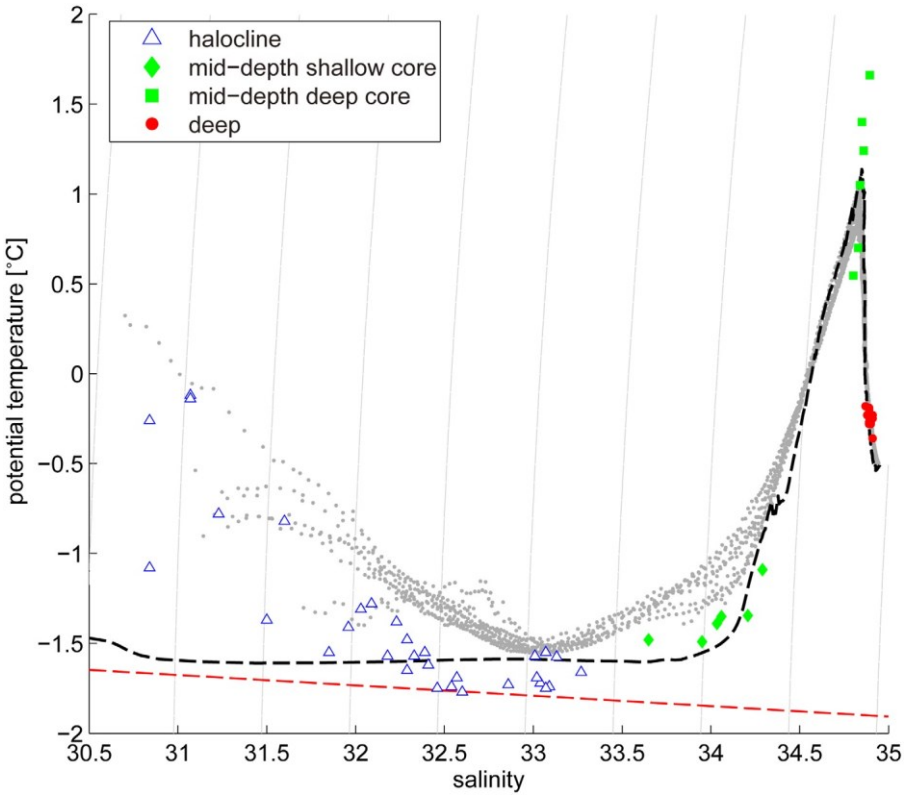

Figure 5. Potential temperature-salinity diagram indicating core water properties of all eddies identified. The red dashed line is the freezing line at zero pressure, and the grey dashed lines are isopycnals (referenced to zero pressure) starting from 25 kg/m^3 on the left with an interval of 1 kg/m^3. Blue triangles represent core T-S for shallow eddies, red dots show deep eddies, and green symbols indicate mid- depth eddies (diamonds for the shallow core, squares for the deep core). The grey dots show typical profiles measured by Mooring B each year from 2003 to 2012 (representative of Canadian Water). The black dashed line represents a typical Eurasian Water profile from CBL2002 data at 80ºN, 177ºW on 31 August 2002.

pairs can also self-propagate [Manucharyan and Timmermans, 2013] (although no dipole pairs are observed here, there remains a low probability [see Manucharyan and Timmermans, 2013] that the observed anticyclones have cyclone partners). Beta-drift in the Canada Basin is smaller than the first mode Rossby wave phase speed given by βR_d^2 (where β is the variation of the Coriolis parameter with latitude and R_d is the deformation radius) [Nof, 1981]. At the location of Mooring B, $R_d \approx 12$ km [see Zhao et al., 2014], and $\beta = 4.8 \times 10^{-12}$ m^{-1} s^{-1} at 78ºN, giving a beta-drift speed of about 0.1 cm/s, an order of magnitude smaller than the background flow field (Figure 1c). Eddies may also translate due to sloping bottom topography, which has an influence similar to the beta-effect [Nof, 1983]. However, this topographic effect is negligible at Mooring B over the abyssal plain where the seafloor slope is less than 0.001. Therefore, it is reasonable to attribute eddy translation past the mooring to the background flow.

The measured horizontal flow field during periods when no eddies are sampled represents the background flow field at the mooring location, time, and depth dependent, with typical values of about 2–5 cm/s. There is a vertical shear in the water column, with the ambient water layer-averaged velocity between 50 and 200 m about twice that in magnitude to the layer-averaged velocity in the more quiescent part of the water column deeper than this (Figure 1c). Shallow eddies are likely to be translated by the fast ambient flow, and deep eddies by the slower flow at depth (for example, Carpenter and Timmermans [2012] considered the average currents over a depth range of 1100–1300 m to estimate advection speeds for the deep eddies). The direction of the flow in both shallow and deep layers tends to be to the northeast at Mooring B in all years, although there is significant variability (on daily time scales) in both speed and direction in both layers. The influence of the double-core eddies is predominantly in the deeper water column (between ~200 and ~1000 m). A reasonable assumption is that the magnitude and direction of the ambient flow is the same over the depth range of both cores, otherwise the cores would be vertically sheared apart by differing advection speeds. To examine this, we consider an 11.25 day temporal mean (11 MMP profiles, and

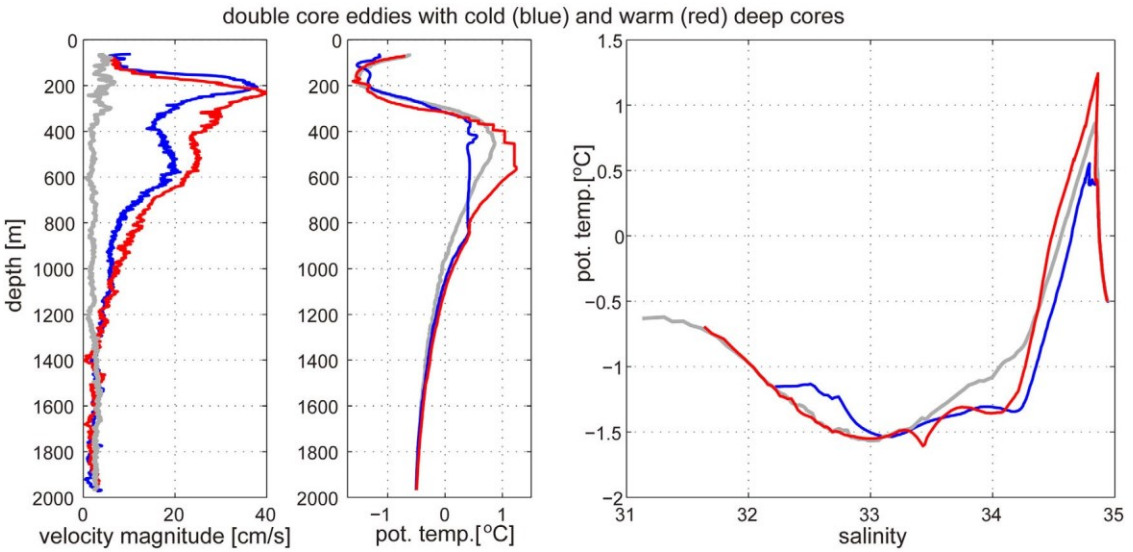

Figure 6. Profiles of (left) velocity magnitude (cm/s), (middle) potential temperature (8C), and (right) potential temperature versus salinity through the centers of two example mid-depth (double-core) eddies; blue lines are for an eddy with an anomalously cold deep core (sampled around 23 July 2004), and red lines for an eddy with an anomalously warm deep core (sampled 23 August 2009). Grey lines show a typical profile in the ambient water at Mooring B.

roughly the time it takes a typical eddy to transit the mooring) and layer-averaged flow fields in a layer between 200 and 350 m depth (the depth range of the shallow core of a double-core eddy) and a layer between 350 and 1000 m depth (the depth range of the deep eddy core). Considering the entire mooring record (excluding eddies), the time-mean background flow varies by less than 0.3 cm/s between these layers (and is in approximately the same direction). Therefore, we assume that the entire double-core eddy structure is translated by the same speed (derived from the layer-averaged 11.25 day temporal mean flow field between 200 and 1000 m preceding the eddy observation that does not show anomalously high speeds (i.e., eddies)). Similarly, for the advection speeds of shallow and deep eddies, the layers over which to compute the background flow (again an 11.25 day temporal mean is taken) are chosen accordingly: 70–170 and 600–1900 m, respectively.

Velocity structure at one depth level through an eddy suggests that the idealized Rankine vortex (i.e., a solid body core where the azimuthal velocity increases with the radius, and outside the core the azimuthal velocity increases inversely with the radius) is an appropriate model for each class of eddy sampled here [see Zhao et al., 2014]. We use this assumption to estimate the radius of an eddy as it transects the mooring (at the estimated advection velocity discussed above) by best fitting the measured azimuthal velocity to a Rankine vortex model (following a similar procedure to Carpenter and Timmermans [2012]). In this way, assuming that the eddy transects the mooring in a straight path (i.e., a chord through the eddy, not necessarily through its center), its radius can only be estimated if two velocity maxima (of opposing signs) are measured. The result of the least squares fit is a grid in the horizontal plane with profile locations relative to an eddy core (center) position (i.e., the MMP profiles in time through the eddy are translated to space). We define the eddy radius R to be the distance between its estimated center location (where the Rankine vortex velocity is zero) and the relative position with the largest azimuthal velocity V_{max}.

Radii of 6 shallow eddies, 10 deep eddies, and 3 mid-depth eddies can be estimated, in general showing larger radii for eddies with deeper cores (Figure 7). The horizontal scales of shallow eddies are around the scale of R_d (rv12 km) at this location, consistent with eddies in the same depth range studied by Zhao et al. [2014]. Two mid-depth double-core eddies have smaller radii in the deeper cores than the shallower cores. The radii of the deep eddies estimated here (between 11 and 19 km) are consistent with the radii ranges estimated by Carpenter and Timmermans [2012] (between 11 and 25 km). The primary source of error in these radii estimates is the estimate of advection velocity. Increasing (decreasing) the advection velocity by 1 cm/s results in an estimated eddy radius that is smaller (larger) by rv30%. Eddy Rossby numbers, which we define as V_{max}=fR (the ratio of the magnitudes of the centrifugal and Coriolis terms in the

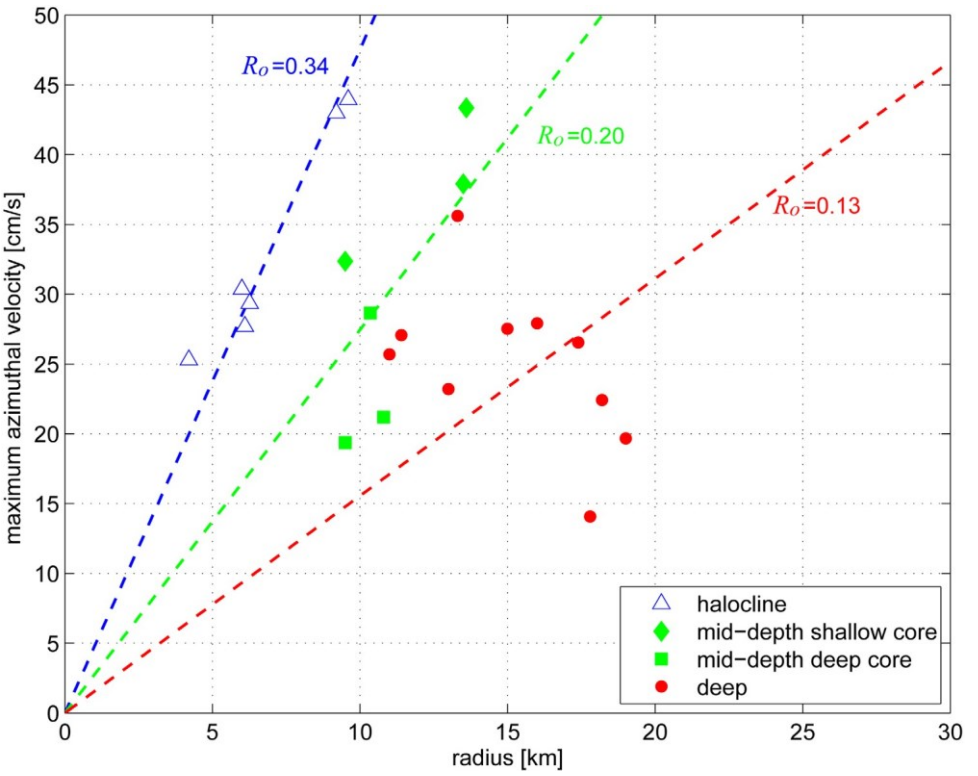

Figure 7. Eddy radii R (km) versus maximum azimuthal velocities V_{max} (cm/s) for all eddies sampled. The slope of the lines indicate Rossby number Ro 5 V_{max}=fR with best fit values for a given eddy class as marked.

cyclogeostrophic momentum balance), range from 0.34 6 0.09 for the shallow eddies to 0.13 6 0.02 for the deep eddies (Figure 7).

4.2. Eddy Vertical Scales

We can now consider eddy horizontal scales estimated above in context with their observed vertical scales (Figure 3). For uniform stratification, the thickness-to-radius (H/R) ratio of a mesoscale eddy is controlled by planetary rotation and stratification with H=R ⁄ f=N. This relationship has been derived in a quasi-geostrophic potential-vorticity conserving framework, and confirmed in both numerical studies and observations. For example, Reinaud et al. [2003] simulated eddies in a range of ambient water conditions, and found that eddies having thickness-to-radius ratios of 0.8f=N were the most stable. Carpenter and Timmermans [2012] showed that deep eddies sampled at Mooring B (with core depths rv1200 m) had thickness-to-radius ratios of about 0.7f=N (for uniform N), defining the eddy top and bottom (to infer H) to be where the azimuthal velocity decays to 10% of its maximum. Zhao et al. [2014] confirmed this relationship for the class of shallow eddies analyzed here.

While uniform stratification may be a good approximation when considering the shallow and deep eddies, when eddies span a region of strongly varying ambient water stratification (as for the double-core eddies), variations in stratification (i.e., N(z)) can influence the adjusted vertical structure of the horizontal velocity and thus the vertical scale of the eddy. We begin by extending the uniform N formalism [see Carpenter and Timmermans, 2012] to account for nonuniform stratification and derive an expression for the resulting steady state vertical structure of the horizontal flow field for a water column characterized by N(z) adjusted to a potential vorticity anomaly.

Quasi-geostrophic potential vorticity (PV) on an f-plane can be expressed as

$$q5\ ^{2}w1\frac{@}{@z}\ \frac{f^{2}\ @w}{N\delta zp^{2}\ @z} \tag{1}$$

for a stream function w with $u = \partial w/\partial y$; $v = -\partial w/\partial x$, and $\zeta = \partial^2/\partial x^2 + \partial^2/\partial y^2$. Following Carpenter and Timmermans [2012], we assume a form for the initial PV $q(x; y; z; t=0) = q_0\delta(z - z_0)$, for $x^2 + y^2 < R^2$, a delta function in the ambient water stratification that is concentrated at the eddy core depth (i.e., the PV anomaly has no thickness initially and an azimuthal velocity concentrated at the eddy core depth, z_0). In the case of a double-core eddy, one core is considered to be the primary core at a level of $z = z_0$, as discussed in the next section. With knowledge of the initial PV, quasi-geostrophic PV conservation allows us to compute the stream function from (1). We assume a solution of the form $w = \hat{w}(z)\exp(ikx + ly)$, where k and l are horizontal wave numbers. Substituting the solution for w into (1) yields

$$\frac{d^2\hat{w}}{dz^2} - \frac{2N_z}{N}\frac{d\hat{w}}{dz} - \frac{K^2N^2}{f^2}\hat{w} = 0 \qquad (z \neq z_0) \tag{2}$$

where N_z is the derivative of N with respect to z, and $K^2 = k^2 + l^2$. Assuming that the solution has the form $\hat{w} = \delta(z)\exp\int \frac{N_z}{N}dz$ yields

$$\frac{d^2\delta}{dz^2} - k^2\delta = 0 \qquad (z \neq z_0) \tag{3}$$

where $k^2 = K^2N^2/f^2 - d(N_z/N)/dz + (N_z/N)^2$. Introducing new coordinates, $W = k^{1/2}\delta$ and $v = \int k\,dz$, (3) may be recast as $d^2W/dv^2 - (1 + d)W = 0$. This can be solved by making the WKB approximation [see e.g., Gill, 1982] wherein $d = (k^{3/2})(d^2k^{-1/2}/dz^2) \ll 1$; the magnitude of d does not exceed 10^{-11} for typical stratification profiles. This has solution $W \propto \exp(-v)$. Returning to original variables, and with boundary conditions $\hat{w}(z) \to 0$ and $\hat{w}(z_0) = q_0$, the vertical structure of the horizontal velocity is then given by

$$\hat{w}(z) = q_0\exp\left[\mathrm{sgn}(z - z_0)\int_{z_0}^{z} \frac{N_z}{N}k\,dz - \ln k^{1/2} + \ln k^{1/2}\Big|_{z=z_0}\right] \tag{4}$$

The vertical influence of the PV anomaly is affected by both the strength of the stratification and the variation in this strength with depth, and this interplay is detailed in the examples described below. For uniform stratification, (4) simplifies to $\hat{w}(z) = q_0\exp(-K|z - z_0|f)$. Taking top and bottom eddy boundaries to be where the velocity decreases to 10% of the maximum velocity gives $H = R = \ln(10)f = N$ [Carpenter and Timmermans, 2012], where we have related K to the horizontal eddy scale R as $K = p = R$.

The typical water column structure in the Canada Basin in the vicinity of Mooring B has two high stratification bands at ~50 and ~200 m, between which the stratification remains relatively strong compared to the deeper water column (Figure 8a shows a typical profile). Deeper than 200 m, the stratification decreases rapidly to ~400 m (around the depth of the Atlantic Water layer), and remains small with increasing depth.

Let us assume that the observed eddies are translated into the Canadian Water stratification and the water column adjusts to the presence of the eddy. This is the case, for example, when a shallow eddy of the type examined in Timmermans et al. [2008] is formed by instability of a surface front in the northern Canada Basin; dense water is subducted from the northern (dense) side of the front into the halocline on the southern side. We examine the observations in context with the prediction (equation (4)) by considering a typical shallow (halocline) eddy (sampled on 25 April 2009 with a core depth of 125 m; Figure 8b), and a typical deep eddy (sampled on 2 July 2007 with a core depth of 1200 m; Figure 8c). With the initial condition being a zero-thickness PV anomaly at the core depth of the eddy in question, the theoretical vertical distribution of horizontal velocity (equation (4)) and the measured velocity structures are generally consistent, and indicate how the stratification limits the vertical influence of the perturbation. For the examples shown, the radius R used in equation (4) is that computed in section 4.1 (with $K = p = R$). Halocline eddies are confined between the two stratification maxima, and the eddy azimuthal velocity decreases rapidly to small values either side of the core depth. On the other hand, deep eddies are centered in the deep water column where the stratification is weak, and this class of eddies has the largest thickness. Although all mid-depth eddies have the double-core structure, we point out here that if an eddy is generated at 400 m (Figure 8d), with higher stratification above than below this depth, there is an asymmetric vertical structure to the horizontal velocity with the velocity decreasing rapidly above 400 m, and more slowly with depth within the relatively weak stratification below 400 m.

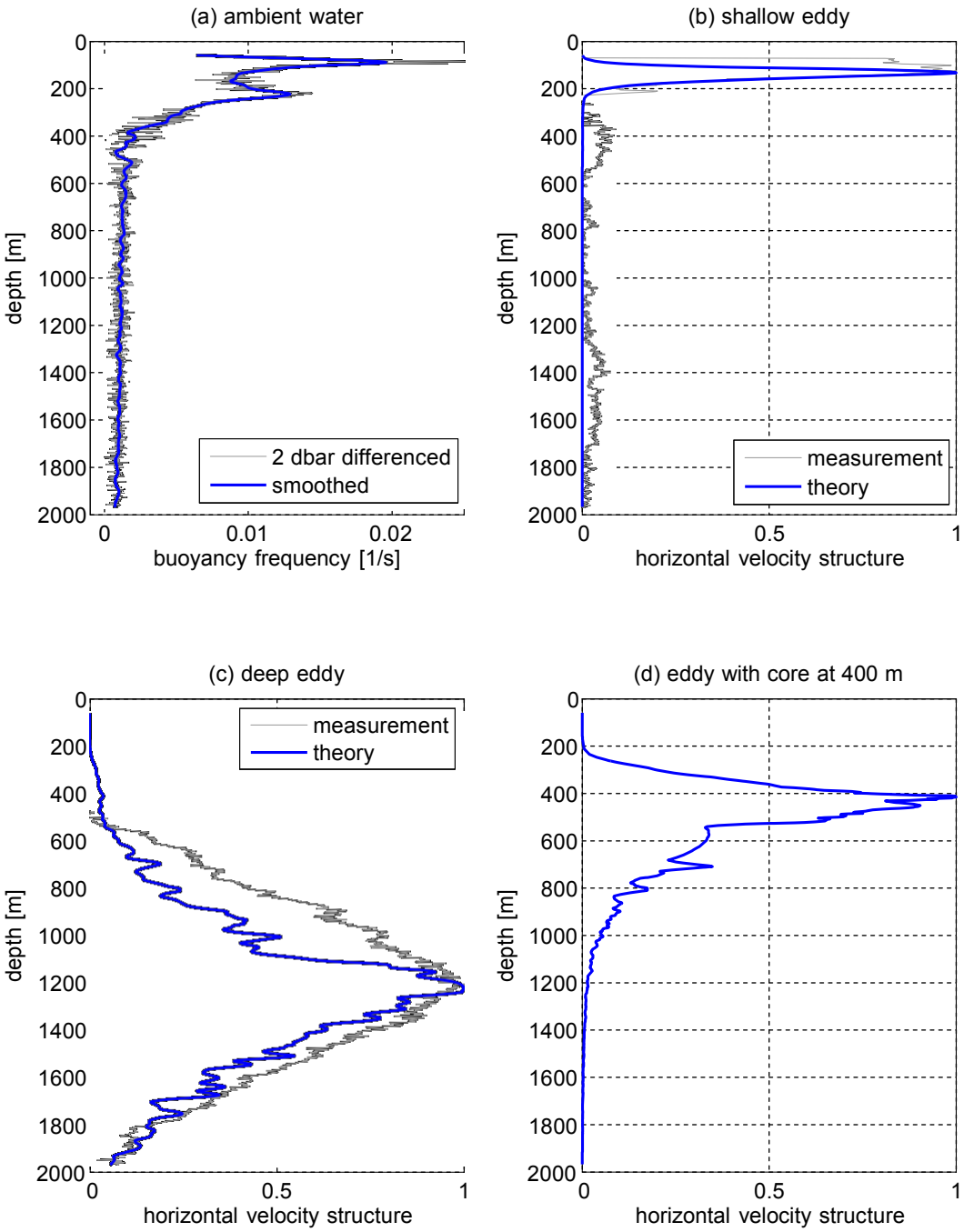

Figure 8. (a) Typical profiles of buoyancy frequency (N(z) (1/s)) in the Canadian Water from Mooring B (grey: computed differencing 2 dbar measurements; blue: smoothed over 11 points). (b, c) Theoretical horizontal velocity structure (blue lines) and measured velocity structure (normalized so that the maximum is 1, grey lines) from representative (b) shallow and (c) deep eddies. The shallow eddy centers at 125 m (measured in April 2009), and the deep eddy centers at 1200 m (measured in July 2007). (d) Theoretical horizontal velocity structure of an eddy with a core at 400 m.

4.2.1. Double-Core Eddies

In contrast to the shallow and deep eddies, double-core eddies, whose fastest azimuthal velocities are located at the depth of their shallow core, are observed in a part of the water column with rapidly weakening stratification with depth. We hypothesize that the shallow core of the double-core eddy is formed by baroclinic instability in the vicinity of the Eurasian/Canadian Water front (near the Chukchi Borderland/Mendeleev Ridge complex, Figure 2). From the thermal wind balance, the slope of the isopycnals at the

front (Figure 2c) indicates that the geostrophic velocity around 200 m depth changes by about 3 cm/s across the front (Morison et al. [1998] showed geostrophic flows associated with this front can reach up to rv4 cm/s). Across the front, the horizontal flow profile is such that the gradient of potential vorticity changes sign, satisfying the necessary conditions for baroclinic instability. When ageostrophic flows (i.e., across-front flows that arise as a result of accelerations and decelerations of the along-front flow) drive Eurasian Water in the halocline to the Canadian Water side of the front, the subducting fluid is compressed and relative vorticity is generated to satisfy PV conservation; in a layered system, for a water column initially with zero relative vorticity and of thickness h_i, this is expressed as $f=h_i/h_f$, where h_f and $f/2V_{max}/R$ are its final thickness and relative vorticity, respectively. For the shallow core of the double-core eddies, we consider the top core to originate from the layer bounded by $33.8 < S < 34.2$, which is of thickness $h_i \approx 43$ m in the Eurasian Water. On the Canadian Water side, it is compressed to a thickness of $h_f \approx 27$ m at around 200 m (Figure 2c), generating a parcel of trapped Eurasian Water with anomalous relative vorticity. The Rossby number of an eddy formed by this process can be estimated as $Ro/V_{max}/fR/f/2f \approx 0.18$, close to the best fit eddy Rossby number of the shallow cores of 0.20 (Figure 7).

The result of the process just described can be considered as a PV anomaly at a depth of 200 m (the depth level of the observed shallow velocity maximum, Figure 9). Following water-column adjustment (equation (4)) in the region of Canadian Water (in the southern Chukchi Borderland, Figure 9a), the velocity first decreases to a minimum and then a second velocity maximum can be generated near the core of the Atlantic Water layer where the stratification is much weaker (rv400 m depth), influencing either cool or warm water at this depth depending on water properties at the eddy generation location (Figure 9b). The predicted vertical structure of the horizontal velocity generally corresponds to that observed in the double-core eddies. Following this adjustment, the entire double-core structure can be advected northeastward by the mean flow to the site of Mooring B. The example above (Figure 8d) demonstrates that an eddy first generated at 400 m does not give rise to a second shallow velocity maximum in this stratification (i.e., the shallow core is primary in the generation).

The generation of double-core eddies reflects adjustment of the water column to a PV anomaly where stratification decreases rapidly with depth to a small value. Water column adjustment is best described in terms of conservation of PV. The PV injection at the shallow eddy core depth introduces isopycnal displacements (Figure 3), which compress the water column above and below the eddy. For a uniformly stratified water column, isopycnal displacements decrease in amplitude away from the eddy core depth (i.e., the extent of water layer compression either side of the eddy reduces), consistent with a decreasing horizontal velocity above and below the core. At the same vertical distance away from the eddy core, isopycnal displacements are larger in a weakly stratified water column compared to a strongly stratified water column (see equation (4)). The response of a nonuniformly stratified water column (e.g., deeper than rv200 m where the stratification decreases rapidly) may be continuously increasing isopycnal displacements with the decrease in stratification to small values; the result is a stretching of the water column (decreasing magnitude of relative vorticity or decreasing horizontal velocity) at first, and a compression of the water layers below (increasing magnitude of relative vorticity). The larger radii of the upper cores compared to the deep cores are consistent with smaller thickness-to-radius ratios where stratification is strongest.

5. Discussion and Summary

A total of 58 mesoscale eddies are classified and analyzed from a decade of velocity, temperature, and salinity measurements from BGEP Mooring B in the northwest Canada Basin. Eddies with deeper core depths have larger horizontal scales, with radii ranging from rv6 km for shallow eddies, rv10 km for mid-depth eddies, and rv16 km for deep eddies. Significant uncertainty in these estimates results from uncertainties in the estimates of advection velocity of an eddy as it transects the mooring. Eddy Rossby numbers range from rv0.34 (shallow eddies) to rv0.20 (mid-depth eddies) and rv0.13 (deep eddies).

Eddies have a range of thicknesses depending on the strength of the ambient water stratification around their core depths, with thicker eddies found in weaker stratification. We have focused our attention on a class of previously unstudied double-core (mid-depth) eddies that have an interesting vertical structure that can be explained by adjustment of the water column to a PV anomaly around the depth of their shallow cores. Considering the location of Mooring B in the vicinity of major water mass boundaries, we propose

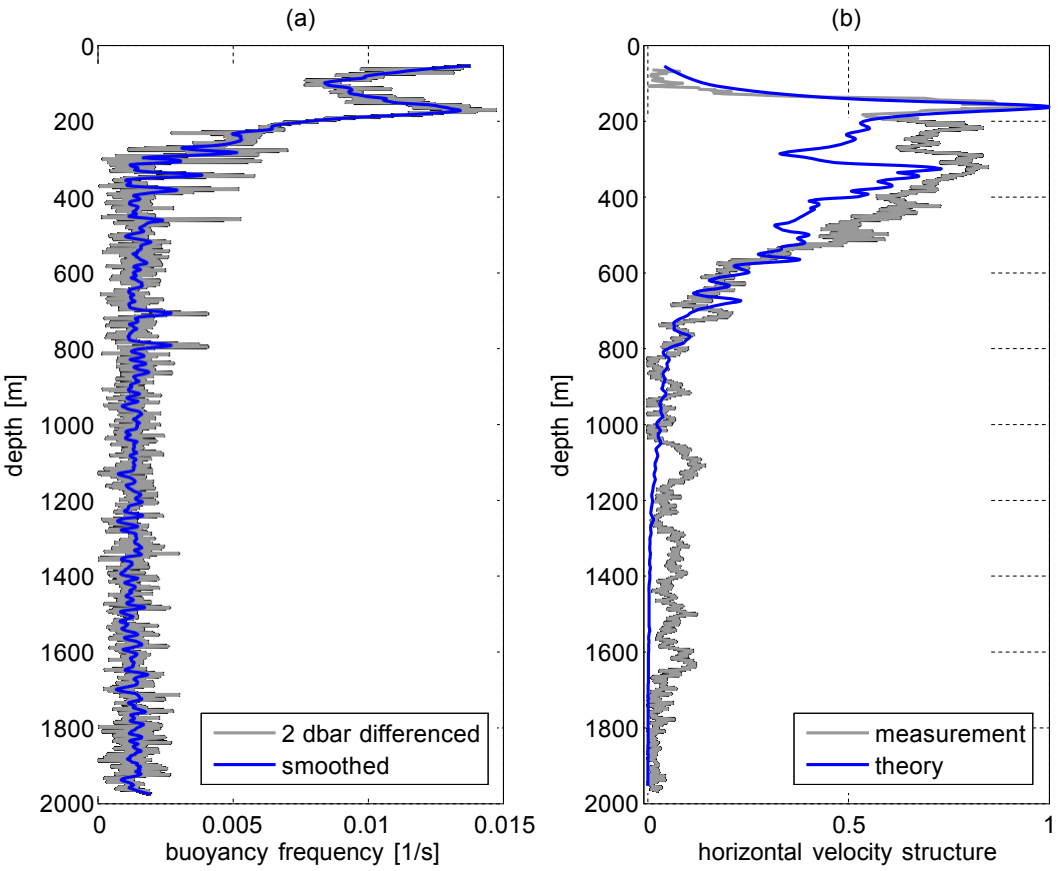

Figure 9. (a) Profile of buoyancy frequency (N(z) (1/s)) in the Canadian Water in the vicinity of a double-core eddy sampled on 23 October 2003 (grey: computed differencing 2 dbar measurements; blue: smoothed over 11 points). (b) Theoretical horizontal velocity structure resulting from adjustment of the water column (with smoothed stratification as in Figure 9a) to a PV anomaly centered at rv180 m (blue line) and measured velocity (normalized so that the maximum is 1, grey line) of a double-core eddy identified on 23 October 2003.

that they originate from the Eurasian Water over the Chukchi Borderland/Mendeleev Ridge complex, where it meets the Canadian Water.

The vertical adjustment of a uniformly stratified portion of the water column to a PV anomaly has been studied before, leading to a relationship between horizontal and vertical scales of eddies [see Carpenter and Timmermans, 2012], a reasonable approximation for the shallow and deep eddies here. We have generalized the derivation to understand dynamical adjustment of a nonuniformly stratified environment for application to the mid-depth eddies that are found in a depth range of rapidly decreasing stratification. The final state of the adjusted water column depends on the structure of the stratification; rapidly decreasing stratification below the halocline causes gradients in water-column compression and relative vorticity generation, giving rise to the double horizontal velocity maxima structure.

The study of double-core eddies sheds light on the possible locations and times where anomalously cool/warm Atlantic Water is found; the deeper core water of the eddy is either cooler or warmer than the Atlantic Water in the vicinity of Mooring B. This anomaly may be associated with unusual hydrographic conditions such as an absence of warm Atlantic Water intrusions, and/or meanders in the Atlantic Water boundary current. The exact pathways and variability of the Atlantic Water (a major source of heat to the Arctic system) are not well known. The presumed source water for the mid-depth eddies is on the Eurasian Water side of the front, in a water mass with higher dissolved oxygen and lower silicate concentrations [Woodgate et al., 2005]. These eddies provide a transport mechanism to the Canadian Water, and demonstrate the communication between the lower Eurasian halocline water and the deeper Atlantic Water. The presence of the double-core eddies suggests that the boundaries of the Beaufort Gyre (separating Eurasian Water and Canadian Water) are unstable and attest to the important role of mesoscale eddies in the regulation of gyre spin-up.

Acknowledgments
Mooring data were collected and made available by the Beaufort Gyre Exploration Program based at the Woods Hole Oceanographic Institution (http://www.whoi.edu/beaufortgyre) in collaboration with researchers from Fisheries and Oceans Canada at the Institute of Ocean Sciences. Special thanks to Andrey Proshutinsky and Rick Krishfield for valuable input. WOD CTD profiles are available from the National Ocean Data Center: https://www.nodc.noaa.gov/OC5/WOD13. CBL2002 data were downloaded from ftp://pscftp.apl.washington.edu/CBL2002Archive. Funding was provided by the National Science Foundation Division of Polar Programs under awards 1107623, 1350046 and 1302884. We appreciate the support and helpful scientific discussions associated with the Forum for Arctic Modeling and Observational Synthesis (FAMOS) and the FAMOS School for Young Arctic Scientists.

References

Aagaard, K., L. K. Coachman, and E. Carmack (1981), On the halocline of the Arctic Ocean, Deep Sea Res., Part A, 28, 529–545, doi:10.1016/0198-0149(81)90115-1.

Carpenter, J. R., and M.-L. Timmermans (2012), Deep mesoscale eddies in the Canada Basin, Arctic Ocean, Geophys. Res. Lett., 39, L20602, doi:10.1029/2012GL053025.

Chelton, D. B., M. G. Schlax, and R. M. Samelson (2011), Global observations of nonlinear mesoscale eddies, Prog. Oceanogr., 91(2), 167–216.

Coachman, L. K., K. Aagaard, and R. B. Tripp (Eds.) (1975), Bering Strait: The Regional Physical Oceanography, Univ. of Wash. Press, Seattle.

D'Asaro, E. A. (1988), Observations of small eddies in the Beaufort Sea, J. Geophys. Res., 93, 6669–6684, doi:10.1029/JC093iC06p06669.

Dmitrenko, I. A., S. A. Kirillov, V. V. Ivanov, and R. A. Woodgate (2008), Mesoscale Atlantic water eddy off the Laptev Sea continental slope carries the signature of upstream interaction, J. Geophys. Res., 113, C07005, doi:10.1029/2007JC004491.

Flor, J.-B. (Ed.) (2010), Fronts, Waves and Vortices in Geophysical Flows, vol. 805, pp. 61–108, Springer, Heidelberg, Germany.

Gill, A. E. (1982), Atmosphere-Ocean Dynamics, 662 pp., Academic Press, San Diego, Calif.

Hunkins, K. L. (1974), Subsurface eddies in the Arctic Ocean, Deep Sea Res. Oceanogr. Abstr., 21, 1017–1033.

Kowalik, Z., and A. Proshutinsky (1994), The Arctic Ocean tides, in The Polar Oceans and Their Role in Shaping the Global Environment, edited by O. M. Johannessen, R. D. Muench, and J. E. Overland, pp. 137–158, AGU, Washington, D. C.

Krishfield, R., J. Toole, A. Proshutinsky, and M.-L. Timmermans (2008), Automated Ice-Tethered Profilers for seawater observations under pack ice in all seasons, J. Atmos. Oceanic Technol., 25(11), 1092–2105, doi:10.1175/2008JTECHO587.1.

Lilly, J. M., and P. B. Rhines (2002), Coherent eddies in the Labrador Sea observed from a mooring, J. Phys. Oceanogr., 32(2), 585–598.

Manley, T. O., and H. L. Hunkins (1985), Mesoscale eddies in the Arctic Ocean, J. Geophys. Res., 90, 4911–4930, doi:10.1029/JC090iC03p04911.

Manucharyan, G. E., and M.-L. Timmermans (2013), Generation and separation of mesoscale eddies from surface ocean fronts, J. Phys. Oceanogr., 43, 2545–2562, doi:10.1175/JPO-D-13-094.1.

Mathis, J. T., R. S. Pickart, D. A. Hansell, D. Kadko, and N. R. Bates (2007), Eddy transport of organic carbon and nutrients from the Chukchi Shelf: Impact on the upper halocline of the western Arctic Ocean, J. Geophys. Res., 112, C05011, doi:10.1029/2006JC003899.

Morison, J., M. Steele, and R. Andersen (1998), Hydrography of the upper Arctic Ocean measured from the nuclear submarine USS Pargo, Deep Sea. Res., Part I, 45(1), 15–38.

Muench, R. D., J. T. Gunn, T. E. Whitledge, P. Schlosser, and W. Smethie Jr. (2000), An Arctic Ocean cold core eddy, J. Geophys. Res., 105, 23,997–24,006, doi:10.1029/2000JC000212.

Newton, J. L., K. Aagaard, and L. K. Coachman (1974), Baroclinic eddies in the Arctic Ocean, Deep Sea. Res. Oceanogr. Abstr., 21(9), 707–719.

Nishino, S., M. Itoh, Y. Kawaguchi, T. Kikuchi, and M. Aoyama (2011), Impact of an unusually large warm-core eddy on distributions of nutrients and phytoplankton in the southwestern Canada Basin during late summer/early fall 2010, Geophys. Res. Lett., 38, L16602, doi:10.1029/2011GL047885.

Nof, D. (1981), On the b-induced movement of isolated baroclinic eddies, J. Phys. Oceangr., 11(12), 1662–1672.

Nof, D. (1983), The translation of isolated cold eddies on a sloping bottom, Deep Sea Res., Part A, 30(2), 171–182, doi:10.1016/0198-0149(83)90067-5.

Padman, L., M. Levine, T. Dillon, J. Morison, and R. Pinkel (1990), Hydrography and microstructure of an Arctic cyclonic eddy, J. Geophys. Res., 21, 707–719, doi:10.1029/JC095iC06p09411.

Pickart, R. S., and G. Stossmeister (2008), Outflow of Pacific water from the Chukchi Sea to the Arctic Ocean, Chin. J. Polar Oceanogr., 10, 135–148.

Pickart, R. S., T. J. Weingartner, L. J. Pratt, S. Zimmermann, and D. J. Torres (2005), Flow of winter transformed Pacific Water into the Western Arctic, Deep Sea. Res., Part II, 52, 3175–3198, doi:10.1016/j.dsr2.2005.10.009.

Plueddemann, A. J., R. Krishfield, T. Takizawa, K. Hatakeyam, and S. Honjo (1998), Upper ocean velocities in the Beaufort Gyre, Geophys. Res. Lett., 25, 183–186, doi:10.1029/97GL53638.

Prater, M. D., and T. B. Sanford (1994), A meddy off Cape St. Vincent. Part I: Description, J. Phys. Oceanogr., 24(7), 1572–1586.

Proshutinsky, A., R. Krishfield, M.-L. Timmermans, J. Toole, E. Carmack, F. McLaughlin, W. J. Williams, S. Zimmermann, M. Itoh, and K. Shimada (2009), Beaufort Gyre freshwater reservoir: State and variability from observation, J. Geophys. Res., 114, C00A10, doi:10.1029/2008JC005104.

Reinaud, J. N., D. G. Dritschel, and C. R. Koudella (2003), The shape of vortices in quasi-geostrophic turbulence, J. Fluid Mech., 474, 175–192, doi:10.1017/S0022112002002719.

Spall, M. A., R. S. Pickart, P. S. Fratantoni, and A. J. Plueddemann (2008), Western Arctic shelfbreak eddies: Formation and transport, J. Phys. Oceangr., 38, 1644–1668, doi:10.1175/2007JPO3829.1.

Timmermans, M.-L., J. Toole, A. Proshutinsky, R. Krishfield, and A. Plueddemann (2008), Eddies in the Canada Basin, Arctic Ocean, observed from Ice-Tethered Profilers, J. Phys. Oceangr., 38, 133–145, doi:10.1175/2007JPO3782.1.

Timmermans, M.-L., et al. (2014), Mechanisms of Pacific Summer Water variability in the Arctic's Central Canada Basin, J. Geophys. Res. Oceans, 119, 7523–7548, doi:10.1002/2014JC010273.

Watanabe, E. et al. (2014), Enhanced role of eddies in the Arctic marine biological pump, Nat. Commun., 5, 3950, doi:10.1038/ncomms4950.

Woodgate, R. A., K. Aagaard, J. H. Swift, K. K. Falkner, and W. M. Smethie (2005), Pacific ventilation of the Arctic Ocean's lower halocline by upwelling and diapycnal mixing over the continental margin, Geophys. Res. Lett., 32, L18609, doi:10.1029/2005GL023999.

Woodgate, R. A., K. Aagaard, J. H. Swift, W. M. Smethie, and K. K. Falkner (2007), Atlantic water circulation over the Mendeleev Ridge and Chukchi Borderland from thermohaline intrusions and water mass properties, J. Geophys. Res., 112, C02005, doi:10.1029/2005JC003416.

Zhao, M., M.-L. Timmermans, S. Cole, R. Krishfield, A. Proshutinsky, and J. Toole (2014), Characterizing the eddy field in the Arctic Ocean halocline, J. Geophys. Res. Oceans, 119, 8800–8817, doi:10.1002/2014JC010488.